J Ginseng Res 45 (2021) 236–245

Contents lists available at ScienceDirect

Journal of Ginseng Research

journal homepage: http://www.ginsengres.org

Research Article

Improvement of antithrombotic activity of red ginseng extract by nanoencapsulation using chitosan and antithrombotic cross-linkers: polyglutamic acid and fucodian

Eun Suh Kim, Ji-Soo Lee, Hyeon Gyu Lee*

Department of Food and Nutrition, Hanyang University, 222, Wangsimni-ro, Seongdong-gu, Seoul 04763, Republic of Korea

ARTICLE INFO

Article history:
Received 24 August 2019
Received in Revised form
1 April 2020
Accepted 3 April 2020
Available online 10 April 2020

Keywords:
Antithrombotic activity
Chitosan nanoparticle
Ionic gelation
Platelet aggregation
Red ginseng
Response surface methodology

ABSTRACT

Background: Red ginseng (RG) extract, especially ginsenoside Rg1 and Rb1 fractions has been reported to have antithrombotic activities. However, gastric instability and low intestinal permeability are considered to be obstacles to its oral administration. We hypothesized that stability, permeability, and activities of RG might be improved by encapsulation within nanoparticles (NPs) prepared with antithrombotic coating materials.

Methods: RG-loaded chitosan (CS) NPs (PF-NPs) were prepared by complex ionic gelation with the antithrombotic wall materials, polyglutamic acid (PGA), and fucoidan (Fu). The concentrations of PGA (mg/mL, X_1) and Fu (mg/mL, X_2) were optimized for the smallest particle size by response surface methodology. Antithrombotic activities of RG and PF-NPs were analyzed using *ex vivo* and *in vivo* antiplatelet activities, *in vivo* carrageenan-induced mouse tail, and arteriovenous shunt rat thrombosis models.

Results: In accordance with a quadratic regression model, the smallest PF-NPs (286 ± 36.6 nm) were fabricated at 0.628 mg/mL PGA and 0.081 mg/mL Fu. The inhibitory activities of RG on *ex vivo* and *in vivo* platelet aggregation and thrombosis in *in vivo* arteriovenous shunt significantly ($p < 0.05$) increased to approximately 66.82%, 35.42%, and 38.95%, respectively, by encapsulation within PF-NPs. For an *in vivo* carrageenan-induced mouse tail thrombosis model, though RG had a weaker inhibitory effect, PF-NPs reduced thrombus significantly due to the presence of PGA and Fu.

Conclusion: PF-NPs contributed to improve the activities of RG not only by nanoencapsulation but also by antithrombotic coating materials. Therefore, PG-NPs can be suggested as an efficient delivery system for oral administration of RG.

1. Introduction

Red ginseng (RG) extract constituents, called ginsenoside derivatives, exhibit broad pharmacological effects on hypertension, diabetes, immunity, stress, fatigue, and cancer [1–3]. In particular, ginsenosides Rg1 and Rb1 have been reported to have significant effects on cardiovascular diseases such as edema, inflammation, myocardial infarction, and cerebral apoplexy [4–6]. In previous studies, ginsenosides Rg1 and Rb1 inhibited excessive platelet aggregation and suppressed thrombosis, which is the first step in the pathogenesis of cardiovascular disease [7–9]. However, instability in gastric environments and low membrane permeability across the intestinal mucosa of ginsenosides Rg1 and Rb1 were indicated as limitations for oral administration [10,11]. To overcome these drawbacks, encapsulation techniques using biocompatible polymers in the form of particles and suspensions have been studied as the promising strategy [12].

Encapsulation is a process used to entrap bioactive compounds within wall materials to prevent degradation, increase bioactivity, and modify physical characteristics [13]. Recently, encapsulation within nanoparticles (NPs) which has the advantage of small size, has been widely used in biopolymer delivery systems to enhance the absorption and uptake efficiency of bioactive materials [14]. Among various methods for nanoencapsulation, ionic gelation based on interactions between oppositely charged materials is regarded as an attractive technique due to the convenient and

* Corresponding author. Department of Food and Nutrition, Hanyang University, 222, Wangsimni-ro, Seongdong-gu, Seoul 04763, Republic of Korea
E-mail address: hyeonlee@hanyang.ac.kr (H.G. Lee).

https://doi.org/10.1016/j.jgr.2020.04.001
p1226-8453 e2093-4947/$ – see front matter

Table 1
Central composite design for the optimization of PF-NP preparation

Run	Coded variable		Decoded variable		Experimental points			
	X_1	X_2	PGA[1]	Fucoidan[2]	Particle size (Y_1)	Zeta potential (Y_2)	Polydispersity (Y_3)	Derived count rate (Y_4)
1	1	1	1.35	0.18	407 ± 27	22.1 ± 1.2	0.258 ± 0.020	198,723 ± 32,490
2	1	−1	1.35	0.06	373 ± 18	21.7 ± 1.7	0.176 ± 0.022	303,170 ± 11,008
3	−1	1	0.85	0.18	325 ± 21	17.3 ± 1.4	0.072 ± 0.020	470,931 ± 42,474
4	−1	−1	0.85	0.06	540 ± 50	15.8 ± 1.7	0.044 ± 0.036	168,700 ± 20,114
5	0	0	1.10	0.12	306 ± 8	18.9 ± 0.9	0.109 ± 0.012	443,870 ± 2,514
6	0	0	1.10	0.12	302 ± 12	18.9 ± 0.8	0.100 ± 0.018	456,063 ± 31,375
7	2	0	1.60	0.12	483 ± 32	23.3 ± 1.1	0.292 ± 0.026	183,600 ± 27,849
8	−2	0	0.60	0.12	774 ± 46	12.4 ± 0.7	0.062 ± 0.019	79,994 ± 6,695
9	0	2	1.10	0.24	310 ± 9	19.2 ± 1.6	0.142 ± 0.017	450,611 ± 23,143
10	0	−2	1.10	0.00	326 ± 15	19.8 ± 2.0	0.099 ± 0.025	299,159 ± 25,807

[1] Concentration of polyglutamic acid (mg/mL).
[2] Concentration of fucoidan (mg/mL).

controllable process [15]. Moreover, natural polysaccharides have been frequently used in formulations intended for oral administration owing to their biodegradable, biocompatible, and nontoxic properties [16]. Chitosan (CS) is one of the most appropriate coating material for ionic gelation because its amine group (NH_2) becomes positively charged (NH_3^+) in the dissolved state and can interact with various negatively charged cross-linkers such as tripolyphosphate (TPP), alginate, and arabic gum [17]. In previous studies, the stability and bioavailability of bioactive materials such as vitamins, polyphenolic compounds, and probiotics were improved by encapsulation within CS NPs which have protection and sustained release properties [18,19].

Existing studies for nanoencapsulation of bioactive materials have been focus on the properties of the NPs as a delivery system. Besides, the biggest distinction from the existing studies of this study is that bioactive materials are used as coating materials for NPs fabrication. In this study, polyglutamic acid (PGA) produced by various strains of *Bacillus*, and fucoidan (Fu) extracted from seaweed were used as cross-linkers for ionic gelation with CS. Owing to its anionic properties in aqueous state, PGA and Fu are capable of generating NPs by cross-linking with positively charged CS [20–22]. Furthermore, PGA and Fu have been reported to prolong blood clotting time and to demonstrate antithrombotic activities [23,24]. Therefore, CS nanoencapsulation with the complex use of PGA and Fu is expected to enhance the antithrombotic activities of RG not only through effect of nanoencapsulation but also owing to the coantithrombotic activities of the coating materials.

This study aimed to investigate the effects of nanoencapsulation by complex use of CS, PGA, and Fu on the antithrombotic activities of RG. RG-loaded NPs were prepared by complex ionic gelation of CS, PGA, and Fu, and the preparation conditions were optimized for the smallest particle size by response surface methodology (RSM). The optimized RG-loaded NPs (PF-NPs) were assessed for solubility, encapsulation efficiency, and antithrombotic activities, including *ex vivo* and *in vivo* antiplatelet activities, *in vivo* carrageenan-induced mouse tail thrombosis, and *in vivo* arteriovenous (AV) shunt rat thrombosis models. Moreover, cytotoxicity assay using Baby hamster kidney fibroblast (BHK 21) cell, and acute toxicity study was also investigated to evaluate the potential toxicity of PF-NPs.

2. Materials and methods

2.1. Materials

RG was supplied by CheonJiYang Co. (Seoul, Korea), and CS (MW 1,000-3,000) was purchased from Kitto Life Co. (Seoul, Korea). PGA (MW 50 kDa) and Fu extracted from *Laminaria japonica* were purchased from Bio Leaders Corp. (Daejeon, Korea) and Haewon Biotech Inc. (Seoul, Korea), respectively. Citrate dextrose solution, Hepes buffer (4-(2-hydroxyethyl)-1-piperazine-ethanesulphonic acid), bovine serum albumin, and carboxymethyl cellulose (CMC) were purchased from Sigma-Aldrich Chemical Co. (St. Louis, MO, USA). Collagen was purchased from Chrono-Log Co. (Havertown, PA, USA).

For the cytotoxicity test, BHK 21 cell was purchased from Korean cell line bank (Seoul, Korea). Dulbeco's modified eagle's medium, L-glutamin, and fetal bovin serum were purchased from Gibco Invitrogen Co. (Grand Island, NY, USA). CMC and 3-(4, 5-dimethylthiazol-2-yl)-2, 5-diphenyltetrazolium bromide (MTT) were purchased from Sigma-Aldrich Chemical Co. (St. Louis, MO, USA). Dimethyl sulfoxide was purchased from Dae-jung Chemical Co. (Seoul, Korea). All other chemicals were reagent grade and were used without further purification.

2.2. Nanoencapsulation of RG extract

CS (0.2 g) and RG (1 g) were completely dissolved in 100 mL distilled water under constant stirring at 1,000 rpm (MS-MP8, Daihan Co., Seoul, Korea), and aqueous solutions of various combinations of PGA and Fu were slowly added into the mixed solution (Table 1). In the presence of CS, PGA, and Fu in the solution, spontaneous cross-linking occurred between the coating materials, resulting in formation of RG-loaded NPs dispersed in aqueous solution.

2.3. Physicochemical properties of NPs

The particle size, zeta potential (ZP), polydispersity index (PDI), and derived count rate (DCR) of NPs were determined by the dynamic light scattering method (Zetasizer Nano ZS, Malvern, Worcestershire, UK).

2.4. Morphology observation

The morphological properties of NPs were investigated by high-resolution transmission electron microscopy (TEM, JEM 2100F, Jeol, Tokyo, Japan). NPs suspension was dropped onto a 200-mesh copper grid and air-dried at 37°C. The dried samples were stained for 30 min using a 2% phosphotungstic acid solution before TEM observation.

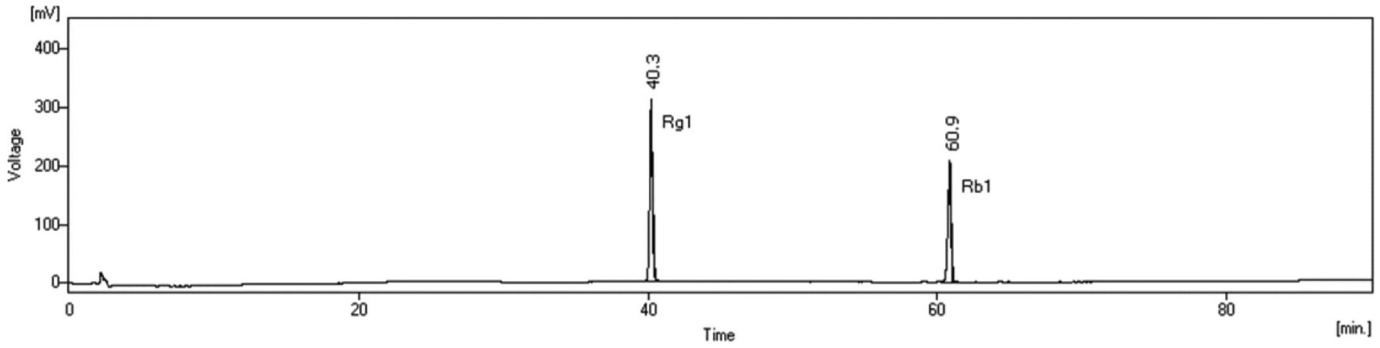

Fig. 1. HPLC chromatogram of the ginsenosides Rg1 (40.3 min) and Rb1(60.9 min). HPLC, high-performance liquid chromatography.

2.5. Experimental design for RSM

The preparation conditions for the optimal physicochemical properties of the PF-NPs were obtained using the predictive equations from RSM [25,26]. The independent variables were the concentrations of PGA (X_1, mg/mL) and Fu (X_2, mg/mL), whereas dependent variables were the physicochemical properties of the PF-NPs, including particle size (Y_1, nm), ZP (Y_2, mV), PDI (Y_3), and DCR (Y_4, kcps). A central composite design was used to fit a second-order equation for two independent variables at five levels (Table 1), and each independent variable was coded based on the experimental data. The complete design was composed of 10 experimental points, including four vertex points, four axial points, and two central points (Table 1). The generalized quadratic polynomial model for predicting the response was as follows:

$$y_n = b_0 + \sum_{i=1}^{2} b_i X_i + \sum_{i=1}^{2} b_{ii} X_i^2 + \sum_{i=1}^{1} \sum_{j=i+1}^{2} b_{ij} X_i X_j$$

where b_0, b_i, b_{ii}, and b_{ij} are the regression coefficients for the intercept, linear, quadratic, and cross-product terms, respectively, and X_i and X_j are the values of the independent variables in the final experiment. The response surface regression procedure of the statistical analysis system program 9.3 (statistical analysis system Institute Inc., Cary, NC, USA) was used to analyze the experimental data and response surfaces. In addition, when the stationary point was a saddle point in the response surfaces, ridge analysis was used to determine the conditions for a set of design variables that maximized (or minimized) an estimated second-order response function. Three-dimensional plots were estimated using Sigma-plot 10.0 (SPSS Inc., Point Richmond, CA, USA), and the predicted and experimental values were compared to assess the validity of the models.

2.6. Determination of ginsenosides

The concentrations of ginsenosides Rg1 and Rb1 were determined using a high-performance liquid chromatography (HPLC) system consisting of two 515 HPLC pumps and a 486 tunable absorbance detector (Waters Corp., Milford, MA, USA). After injecting 50 μL of the samples, the ginsenoside derivatives were eluted with a gradient of (A) distilled water and (B) acetonitrile using pumps with a degasser (ERC-3215α, ERC Inc., Kawaguchi, Japan). Separation was performed in a YMC-Pack Pro C_{18} column (4.6 × 250 mm, 5 μm, YMC Co., Ltd., Kyoto, Japan) at 40°C using a column heater (CH-500, Eppendorf, Hamburg, Germany). The ginsenosides Rg1 and Rb1 were detected by measuring UV absorbance at 203 nm. The gradient conditions of the mobile phase at a flow rate of 1.6 mL/min were as follows: 0 min, 80% A; 5 min, 80% A; 13 min, 75% A; 85 min, 55% A; 90 min, 10% A; 95 min, 55% A; 98 min, 80% A; and re-equilibration from 98 to 100 min with 80% A [27]. The chromatographic peaks at 40.3 and 60.9 min were identified as ginsenosides Rg1 and Rb1, respectively, by analogy with the HPLC peaks of commercial standards (Fig. 1).

2.7. Solubility

The solubility of ginsenosides Rg1 and Rb1 was analyzed after filtering the RG and PF-NP suspensions through nylon membrane filters with a pore size of 0.45 μm to remove the insoluble ingredients [28]. The completely dissolved ginsenosides were quantified by referencing the standard curve for commercial ginsenosides.

2.8. Encapsulation efficiency

The encapsulation efficiency of the NPs was calculated using the following equations with the amount of nonencapsulated-free ginsenosides Rg1 and Rb1 in the supernatant after ultracentrifugation (Optima TL, Beckman, Fullerton, CA, USA) at 30,000 × g for 30 min [29].

$$\text{EE}\ (\%) = \frac{\textit{Actual amount of ginsenoside in NPs}}{\textit{Theoretical amount of ginsenoside in NPs}} \times 100 \qquad (1)$$

2.9. In vitro release properties

Simulated gastric fluid (SGF) and simulated intestinal fluid (SIF) were prepared by adjusting the suspension of PF-NPs to pH 1.2 and 6.8 with 0.1 M HCl and NaOH, respectively [30]. The PF-NPs were continuously exposed to SGF for 2 h and SIF for 4 h at 37°C. After exposure to both SGF and SIF, the PF-NPs suspensions were collected and centrifuged at 15,000 × g for 30 min. The ginsenoside in the supernatant was quantified by HPLC. The ginsenoside release rate was calculated using Eq. (2):

$$\text{Release rate}(\%) = \frac{\textit{Amount of ginsenosides released from PF} - \textit{NPs}}{\textit{Amount of ginsenosides initially entrapped in PF} - \textit{NPs}} \times 100 \qquad (2)$$

2.10. Antithrombotic activity

2.10.1. Animals

For *ex vivo* experiments, New Zealand white rabbits were purchased from Koatech Co. (Pyongtaek, Korea), housed at a temperature of 24 ± 1°C and humidity of 55 ± 5%, and provided laboratory food pellets and tap water. All animals and animal procedures were approved by the Institutional Animal Care and Use Committee (IACUC) and the laboratory animal care guidelines of Hanyang University, respectively. Five-week-old male ICR mice (25 ± 2 g) for the *in vivo* carrageenan-induced mouse tail thrombosis model and male Sprague–Dawley rats (200–250 g) for the *in vivo* platelet aggregation assay and AV shunt thrombosis model were purchased from Orient Bio, Inc. (Seongnam, Korea). The mice and rats were housed at a temperature of 22 ± 2°C and humidity of 55 ± 5% with a 12 h light–dark cycle and were acclimatized with standard chow for one week before use. All animal experiments were performed in accordance with the IACUC guidance of Daejeon University.

2.10.2. Ex vivo platelet aggregation assay

The platelet aggregation assay was performed by the turbidimetry method using an aggregometer (Chrono-log 490, Chrono-log Co., Havertown, PA, USA). Whole blood from the rabbit ear artery was collected into anticoagulant citrate dextrose solution and centrifuged (Combi 408, Hanil Co., Seoul, Korea) at 230 × g for 10 min to obtain platelet-rich plasma (PRP). The PRP was then centrifuged again at 800 × g for 15 min, and the precipitated platelets were washed with Hepes buffer (137 mM NaCl, 2.7 mM KCl, 1 mM $MgCl_2$, 5.6 mM glucose [GLU], and 3.8 mM Hepes, pH 6.5) containing 0.35% bovine serum albumin and 0.4 mM ethylene glycol-bis(13-aminoethyl ether)-N,N,N'N'-tetraacetic acid. The washed platelets were adjusted to a concentration of 4×10^8 cells/mL in Hepes buffer (pH 7.4) and spun at 1,000 rpm at 37°C in the aggregometer. The washed platelets were treated with RG and PF-NP suspensions that were adjusted to pH 2 using 0.1 M HCl. After preincubation for 3 min, 5 μg/mL of collagen was added as an agonist to induce platelet aggregation [31].

2.10.3. In vivo platelet aggregation

Freeze-dried RG and PF-NPs were dispersed in 0.25% (w/v) CMC solution and orally administered to rats at 300 mg/kg of body weight at the same time for three consecutive days. PRP was obtained by centrifuging whole blood at 230 × g for 15 min, and platelet poor plasma was obtained by centrifuging PRP at 800 × g for 15 min. After administration for 1 h, PRP was collected and adjusted to 3×10^8 platelets/mL with platelet poor plasma. Platelet aggregation was induced by 10 μg/mL collagen and evaluated in the aggregometer [31].

2.10.4. In vivo carrageenan-induced mouse tail thrombosis model

Freeze-dried RG and PF-NPs dispersed in 0.25% (w/v) CMC solution were orally administered to mice at a dose of 300 mg/kg. After administration for 1 h, 40 μL of 1% sterile carrageenan (Type I) in physiological saline was injected into the right hind paw of each mouse. The inhibitory effects of the samples on thrombosis were measured by the length of infarction in the tail at 24, 48, and 72 h. Heparin and aspirin were used as positive controls with doses of 100 IU/kg and 20 mg/kg, respectively [32].

2.10.5. In vivo AV shunt model

Freeze-dried RG and PF-NPs dispersed in 0.25% (w/v) CMC solution were orally administered to rats at a dose of 300 mg/kg for three consecutive days. Two hours after the final dose, the rats were anesthetized using pentobarbital sodium salt (60 mg/kg, intraperitoneally). The left jugular vein and the right carotid artery were cannulated with two saline-filled catheters. The catheters were then connected to a polyethylene tube with a saline-filled shunt, which consisted of cotton thread (0.25 mm diameter) and tygon tube (2 mm internal diameter). The antithrombotic effects of the samples in the AV shunt model were evaluated based on the weight of the associated thrombus on the cotton thread after 15 min of extracorporeal circulation [33].

2.11. Toxicity

2.11.1. Cytotoxicity

Cell viability assessing the protective and cytotoxic effects of the PF-NPs was analyzed by MTT assay [34]. Viable BHK 21 cells were seeded (180 μL) in 96-well plate with cover-glasses on the bottom at a density of 1.0×10^4 cells/well and treated with 20 μL PF-NPs suspension at concentration varied from 0.2 to 1.0 mg/mL. After incubation for 24 h, 20 μL MTT solution was added to each well and incubated for further 4 h to promote formation of purple formazan derived from reaction between yellow tetrazolium bromide and mitochondrial succinate dehydrogenase in viable cells. The supernatant was removed through centrifugation (Combi 408, Hanil Co., Seoul, Korea) at 400 × g for 5 min and dimethyl sulfoxide was added for complete dissolution of the formazan crystal. Cell viability was analyzed by reading UV absorption of formazan produced at 540 nm using ELISA microplate reader (ELx800UV, Bio-Tek Instrument Inc., Windoski, VT, USA).

2.11.2. Acute toxicity study

Each of twenty male and female Sprague–Dawley rats was purchased from Orient Bio. Inc. (Seongnam, Korea). All rats were kept at a temperature of 23 ± 3°C and relative humidity of 30-70% with a 12 h light–dark cycle and provided laboratory food pellets and fresh tap water. All animals were approved by the IACUC, and the procedures were performed in accordance with the guidelines of Organization for Economic Co-operation and Development Principles of Good Laboratory Practice by Ministry of Food and Drug Safety.

The animals were divided into one control group and 3 treated groups; five male and female rats were randomly contained in each group. Dose levels of freeze-dried PF-NPs were selected as 3,000, 1,000, and 300 mg/10mL/kg/day in accordance with the recommendation of Ministry of Food and Drug Safety guidelines. The samples were dissolved in 1% CMC (w/v) solution and orally administered to rats using a sonde attached to a 1 mL syringe after 18 h of overnight fasting (except for water). Feed and water were restricted for 3 h after administration of the samples.

2.12. Statistical analysis

All data were collected from experiments performed in triplicate and are expressed as mean ± standard deviation. The significant differences ($p < 0.05$) among the corresponding mean values were determined using one-way analysis of variance followed by Duncan's multiple comparison test (SPSS 12.0.1, SPSS Inc., Chicago, IL, USA).

3. Results and discussion

3.1. Effects of independent variables on properties of PF-NPs

Because NPs prepared by ionic gelation are formed through the interaction between oppositely charged materials, the characteristics of the CS NPs are greatly affected by the mixing ratio of the coating materials [35]. Moreover, the most advantageous property of the NPs is the large surface area/volume ratio achieved by small

particle size, which can increase solubility, biodelivery, and absorption at the site of digestion [36,37]. In the previous study, NPs with small particle size, good dispersibility, and uniformity were fabricated at a specific mixing ratio of CS and TPP, whereas the characteristics of NPs became worse as the concentration of TPP increased or decreased relative to this ratio [15]. Because the PGA and Fu used in this study are both anionic materials, they react with the cationic CS in a competitive and complementary manner during PF-NP formation. Therefore, to determine the most effective preparation conditions for the smallest particle size, the mixing ratio of PGA and Fu was varied under a constant concentration of CS. Based on the results of our previous study, the concentrations of PGA and Fu affected the particle properties at 2 mg/mL CS and 10 mg/mL RG [27]. Moreover, the concentration ranges of PGA and Fu that had significant influence on properties while maintaining the characteristics of the NPs were found to be 0.6 to 1.6 mg/mL and 0.002 to 0.24 mg/mL, respectively. Therefore, the concentrations of PGA and Fu were selected as independent variables for optimization of PF-NPs using RSM in this study.

The independent variables were coded at five levels based on the central composite design (Table 1). The dependent variables particle size (Y_1), ZP (Y_2), PDI (Y_3), and DCR (Y_4) were analyzed in 10 experiments, which were generated by combining various conditions for the two independent factors at five levels each (Table 1). The smallest and largest sizes (302.7 and 773.7 nm) were obtained for PF-NPs in experiments 6 and 8, respectively. The ZP ranged from 12.4 to 23.3 mV (experiments 8 and 7, respectively), and the DCR ranged from 79,994 to 470,931 kcps (experiments 8 and 3, respectively). The PDI values in all experiments ranged from 0.062 to 0.292, remaining below 0.3, which is regarded as the value necessary for satisfying particle distribution and uniformity [38]. Therefore, all of the experiments within the design resulted in acceptable physicochemical properties of the NPs and can be considered adequate preparation conditions for optimizing the PF-NPs by RSM.

Regression model equations were generated for the dependent variables based on the observed values from the 10 experiments performed using the model, and the regression coefficients for the dependent variables were calculated from the experimental data obtained by multiple linear regressions (Table 2). The multiple regression coefficients (R^2) of the models for particle size, ZP, PDI, and DCR were 0.9369, 0.9840, 0.9623, and 0.8916, respectively, indicating that the model fit a significant amount of the variability in response. Particle size was significantly affected by negative linear and positive quadratic effects of the PGA ($p < 0.01$) and negative linear effects of Fu ($p < 0.1$). The interaction effect between PGA and Fu (X_1X_2) had a significantly positive influence on response ($p < 0.1$). The effect of PGA on the DCR had the opposite trend to that of particle size. There were significant positive linear and negative quadratic effects of PGA on DCR at $p < 0.01$ and $p < 0.05$, respectively. The linear effect of Fu was also found to be significantly positive at $p < 0.05$. Moreover, the interaction effect (X_1X_2) had a significantly negative impact on the response at $p < 0.1$. With respect to ZP and PDI, only PGA had positive linear and quadratic effects on the response at $p < 0.05$, respectively. Based on the regression coefficients, PGA is believed to be the most effective factor influencing the dependent variables, while Fu contributed little.

3.2. Optimization of PF-NP preparation conditions

Response surface plots were generated from the measured responses based on the models used to predict optimum values and analyze relationships between the independent and dependent variables (Fig. 2). The three-dimensional plot of particle size versus PGA and Fu concentration confirmed the results of the regression coefficient analysis (Fig. 2a). As aforementioned, both anionic materials, PGA and Fu, can form NPs in the presence of cationic CS, and the concentration ratio of PGA and Fu had a significant effect on particle size. PGA showed significantly stronger effects than Fu, demonstrating negative linear and positive quadratic effects on particle size. Canonical analysis for determining the optimal conditions revealed that the predicted stationary point for particle size was the saddle point. The minimum particle size was located at the intersection point of PGA and Fu concentrations, which ranged from approximately 1.0 to 1.4 mg/mL and from 0.09 to 0.18 mg/mL, respectively. Therefore, a ridge analysis was performed to determine the critical levels for the maximum and minimum responses. The predicted minimum (268.8 ± 64.6 nm) and maximum (795.3 ± 58.9 nm) NPs sizes were observed when PGA and Fu concentrations were 1.332 and 0.014 mg/mL, and 0.628 and 0.081 mg/mL, respectively.

The effects of PGA and Fu concentrations on ZP are displayed graphically in Fig. 2b. ZP, defined as the electrostatic potential of NPs surfaces in aqueous solution, is regarded as the main parameter for the stability of NPs [39]. Because stable NPs can be prepared by increasing the cross-linking strength between the coating materials, the three-dimensional plot revealed the tendency for ZP to increase with increases in PGA and Fu concentrations at a constant CS concentration. However, only PGA was found to have significant

Table 2
Regression coefficients of the predicted second-order model for the response variables

Model parameter	Particle size (Y_1) ($R^2 = 0.9369$)		Zeta potential (Y_2) ($R^2 = 0.9840$)		Polydispersity (Y_3) ($R^2 = 0.9623$)		Derived count rate (Y_4) ($R^2 = 0.8916$)	
	Coefficient	S.E.[1]	Coefficient	S.E.	Coefficient	S.E.	Coefficient	S.E.
Constant	2,691.62***	378.06	−0.52	4.08	0.26	0.16	−2,095,958**	474,898
Linear								
X_1[2]	−3,519.05***	542.36	23.37**	5.85	−0.46	0.23	3,469,777***	681,289
X_2[3]	−4,986.43*	2,286.62	13.22	24.65	−0.93	0.98	9,086,937**	2,872,355
Quadratic								
X_1^2	1,272.14***	222.09	−4.70	2.39	0.28**	0.10	−1,196,938**	278,986
X_2^2	523.31	3,855.81	32.99	41.56	0.90	1.65	−3,899,058	4,843,506
Cross-product								
X_1X_2	4,150.00*	1,884.75	−18.33	20.32	0.90	0.81	−6,777,967*	2,367,545

*** Significant at $p < 0.01$.
** Significant at $p < 0.05$.
* Significant at $p < 0.1$.
[1] Standard error.
[2] Concentration of polyglutamic acid.
[3] Concentration of fucoidan.

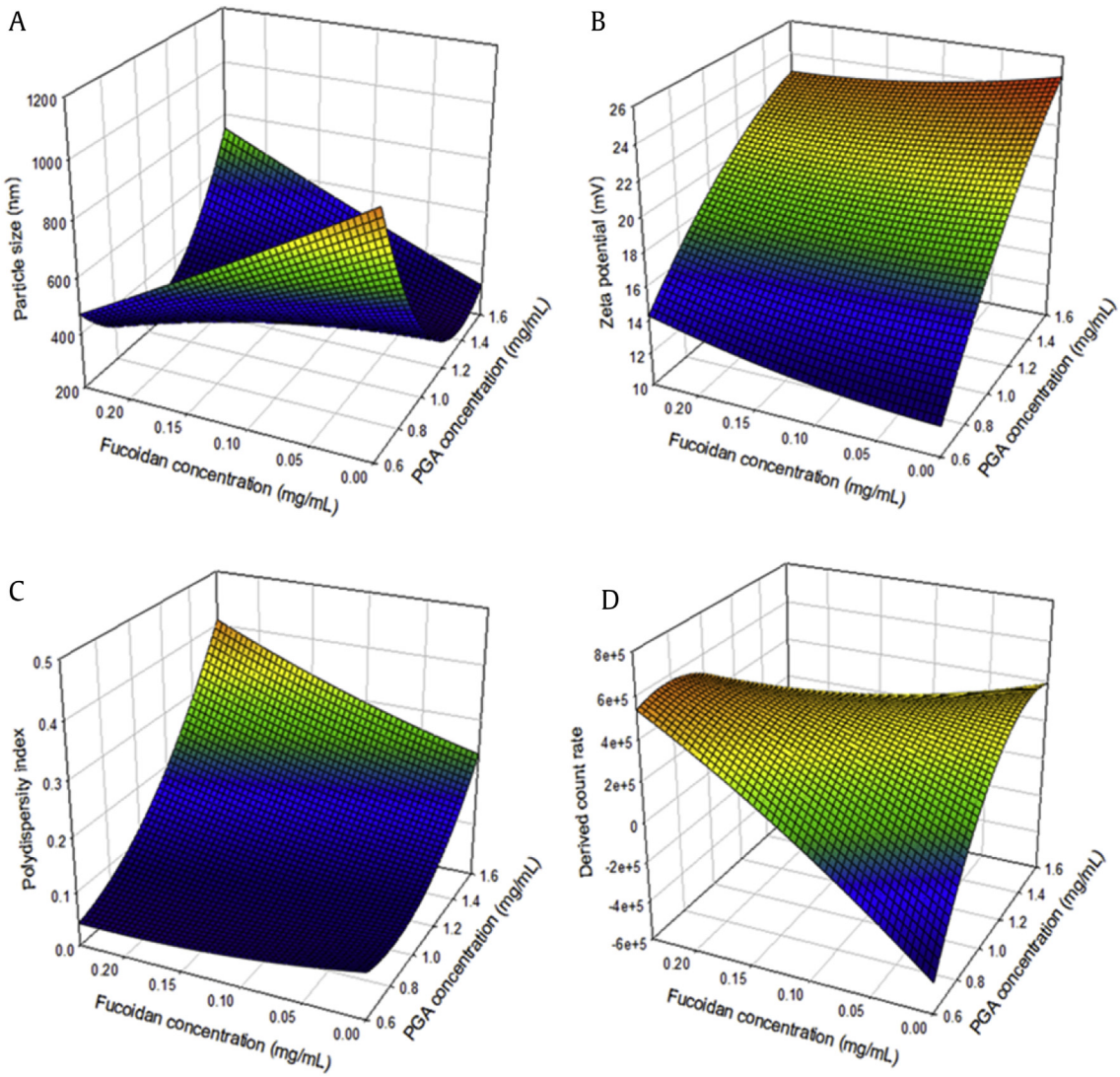

Fig. 2. Three-dimensional response surface plots for effects of PGA (X_1) and fucoidan (X_2) concentrations on (A) particle size (Y_1), (B) zeta potential (Y_2), (C) polydispersity index (Y_3), and (D) derived count rate (Y_4).

positive linear effects on ZP, as shown in the regression coefficient analysis. Because the stationary point was a saddle point, a ridge analysis was performed to determine the critical levels of ZP. The minimum (12.48 ± 0.56 mV) and maximum (23.57 ± 0.64 mV) ZP values were observed when PGA and Fu concentrations were 0.605 and 0.104 mg/mL, and 1.572 and 0.081 mg/mL, respectively.

The graphical analysis of the PDI also confirmed the results of the regression coefficient analysis, showing that the quadratic term of PGA had a significant negative effect on PDI, whereas Fu had no significant effects (Fig. 2c). The PDI represents NPs uniformity because it indicates the particle size distribution, and a value lower than 0.3 is considered highly homogeneous [38]. In this study, highly homogeneous NPs with PDI values lower than 0.3 were found for all PGA and Fu proportions except for the intersection where PGA varied from approximately 1.5 to 1.6 mg/mL and Fu varied from approximately 0.15 to 0.25 mg/mL. Because the stationary point was the minimum point, the PDI decreased with decreases in both PGA and Fu. However, below a certain concentration of PGA, decreasing the Fu concentration did not further decrease the PDI because the minimum response was located at less than approximately 0.7 mg/mL of PGA. The minimum (0.045 ± 0.045) and maximum (0.324 ± 0.025) PDI values were observed when PGA and Fu concentrations were 0.635 and 0.164 mg/mL, and 1.575 and 0.158 mg/mL, respectively.

The amount of NPs in a colloidal suspension can be roughly estimated from the DCR [40]. In support of the results of the regression coefficient analysis, the response surface for the effect of varying PGA and Fu concentrations on the DCR exhibited a trend that was opposite to that of particle size (Fig. 2d). It can be assumed that a decrease in particle size correlates with an increase in the number of single NPs in certain concentrations of coating materials [41]. The minimum (−55,975 ± 84,974 kcps) and maximum (539,465 ± 80,365 kcps) DCR values were predicted when PGA and Fu concentrations were 0.683 and 0.054 mg/mL, and 0.876 and 0.227 mg/mL, respectively. The predicted minimum DCR appeared to be less than 0, which is technically impossible because DCR cannot have a negative value. This result can be considered to be an unavoidable statistical error in the RSM software, which only depends on the value to make its prediction; further investigation is necessary to minimize this error [42].

These results confirmed again that PGA effectively influenced the properties of NPs, and that PGA was a more effective factor than

Table 3
Experimental values for the response variable

Charateristics	The smallest PF-NPs
Optimum conditions	
Polyglutamic acid (mg/mL)	1.332
Fucoidan (mg/mL)	0.014
Observed values	
Particle size (nm)	286.7 ± 36.6
Zeta potential (mV)	−21.5 ± 1.0
Polydispersity index	0.147 ± 0.019
Derived count rate (kcps)	231,144 ± 10,847
Encapsulation efficiency (%)	20.78 ± 0.20
Ginsenoside release in SGF[1] (%)	31.47 ± 6.17
Ginsenoside release in SIF[2] (%)	67.57 ± 9.81

SGF, simulated gastric fluid; SIF, simulated intestinal fluid.
[1)] Exposure of the PF-NPs to simulated gastric fluid (pH 1.2) for 2 h.
[2)] Exposure of the PF-NPs to simulated intestinal fluid (pH 6.8) for 6 h.

Fu. Moreover, the results confirmed that the particle characteristics of PDI, ZP, and DCR were acceptable for all of the RG-loaded NPs prepared within the concentration ranges of PGA and Fu. Therefore, the preparation conditions of the NPs were selected for the smallest particle size, which is considered to be the most important factor in the effectiveness of NPs, and was applied to evaluate their antithrombotic activity.

3.3. Verification experiments

The preparation conditions of the PF-NPs were optimized for the smallest particle size, and PF-NPs at these conditions were determined to verify the predictive capacity of the model (Table 3). The formation of PF-NPs could be demonstrated by morphological investigation by TEM which revealed the layer by layer formation of spherical particles from the cores to the edges of the complex molecular aggregates (Fig. 3). The measured (286.7 ± 36.6 nm) and predicted (268.8 ± 64.64 nm) particle sizes were found not to be statistically different at a 95% confidence level, confirming the validity of the model. The other physicochemical properties of the smallest PF-NPs determining the effective particle formation state—ZP, PDI, and DCR values of −21.5 mV, 0.147, and 231,144 kcps, respectively—were also acceptable as mentioned previously.

Furthermore, the characteristics of PF-NPs as a biodelivery system for ginsenosides were also evaluated (Table 3). The ginsenosides Rg1 and Rb1 were encapsulated within the PF-NPs with an efficiency of 20.78 ± 0.20%. The aqueous solubility of ginsenoside Rg1 and Rb1 was significantly increased by approximately 26.44%, from 110.37 ± 3.05 to 135.70 ± 0.34 mg/mL, after encapsulation in the PF-NPs. Moreover, *in vitro* ginsenoside release profile from PF-NPs was observed to be sustained in simulated gastrointestinal (GI) tract. Moreover, *in vitro* release of ginsenosides from the PF-NPs demonstrated sustained release characteristics in simulated GI tract. Ginsenoside release rate from the PF-NPs was 31.47 ± 6.17% after 2 h of SGF exposure, followed by 67.57 ± 9.81% after continuous exposure to SIF for 6 h.

3.4. Ex vivo and in vivo platelet aggregation

Platelet aggregation, the primary step of the entire blood coagulation mechanism, is believed to occur mainly via three pathways: release of adenosinediphosphate (ADP), formation of thromboxane A_2, and platelet activation [43]. These pathways are induced by endogenous agonists such as collagen, arachidonic acid, and ADP. Collagen is involved in all of the reaction pathways, whereas arachidonic acid and ADP activate only the first two events [44]. Therefore, the results of the collagen-induced platelet aggregation test indicate that RG has significant effects on the general mechanism of platelet aggregation.

The *ex vivo* collagen-induced platelet aggregation ratio in the presence of free RG and PF-NPs in the acidic condition of pH 2 was 22.3 ± 1.2% and 7.4 ± 3.8%, respectively (Fig. 4a). RG had significant inhibitory effects on platelet aggregation compared with controls (36.5 ± 7.5%), and the inhibitory activity of RG significantly increased when encapsulated in PF-NPs. The results were confirmed by *in vivo* experiments, in which the PF-NPs showed significantly greater inhibition of platelet aggregation (26.8 ± 1.9%) compared with that of free RG (41.5 ± 3.5%). The stronger effect seen with PF-NPs can be explained by the increased solubility of ginsenosides in active form and the sustained release of entrapped ginsenosides in simulated GI tract. These properties could lead to improved stability of RG in acidic environments such as gastric juice, thereby resulting in higher bioactivity and bioavailability of ginsenosides during digestion [45,46].

3.5. In vivo carrageenan-induced mouse tail thrombosis model

Thrombus appeared as a red wine–colored dry necrotic region in the end of the tail after 48 h of subcutaneous carrageenan injection. The mean thrombus lengths of the control, heparin, aspirin, and free RG groups were 2.14 ± 1.55, 1.46 ± 0.72, 2.98 ± 1.62, and 1.87 ± 0.72 cm, respectively (Fig. 4b). No significant effects of aspirin and free RG on carrageenan-induced thrombosis were observed at doses of 20 mg/kg and 300 mg/kg, respectively, whereas heparin showed significantly greater inhibitory activity.

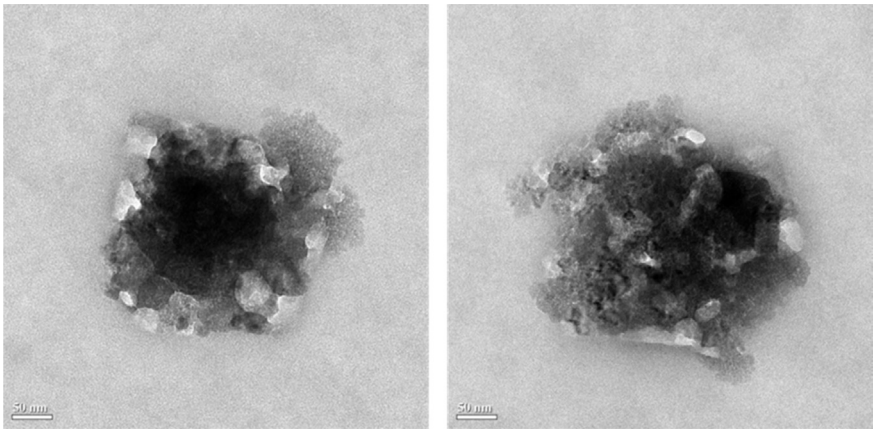

Fig. 3. TEM image of the smallest optimized PF-NPs prepared with 1.332 mg/mL PGA and 0.014 mg/mL Fu. TEM, transmission electron microscopy.

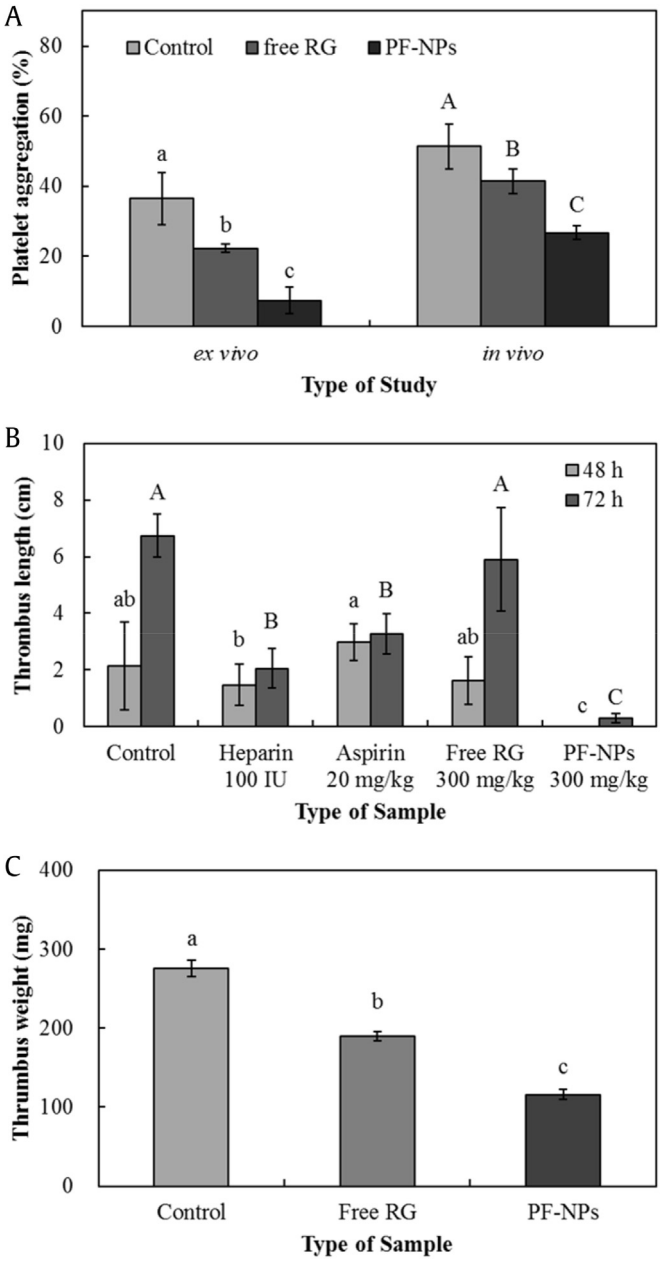

Fig. 4. Inhibitory activities of (A) *ex vivo* and *in vivo* platelet aggregation, (B) *in vivo* carrageenan-induced mouse tail thrombus, and (C) *in vivo* AV shunt thrombus of RG and PF-NPs. All data are presented as mean ± standard deviation, and different capital and lowercase letters indicate significant differences ($p < 0.05$). RG, red ginseng; AV, arteriovenous.

Thrombus was not observed in the PF-NP group. With the passage of time, the mean thrombus length for each group increased significantly; the mean thrombus lengths of the control, heparin, aspirin, free RG, and PF-NP groups after 72 h were 6.74 ± 0.75, 2.04 ± 3.27, 3.27 ± 0.71, 5.89 ± 1.83, and 0.30 ± 0.16 cm, respectively. The greatest thrombus length was more than 6 cm and was observed in both the control and free RG groups, while the positive control groups, heparin and aspirin, showed significantly lower thrombus production. In the group treated with PF-NPs, thrombus formation slightly increased after 72 h, a significantly greater inhibition of thrombosis compared to the other groups.

A carrageenan-induced thrombosis model has been widely studied for evaluating antithrombotic materials due to many advantages, including a simple and easy application method that does not kill the animals and the ability to accurately quantify thrombus by visual observation [47]. After carrageenan injection, inflammation is generated in local blood vessels, leading to secretion of inflammation factors, which cause damage to endothelial blood vessel cells and interrupt their function. The endothelial cell injury that results from the inflammation of local blood vessels can lead to the formation of intravascular thrombus. Furthermore, carrageenan activates the Hageman factor (factor XII) of the intrinsic coagulation pathway, which is part of the secondary step of the blood coagulation mechanism, resulting in acceleration of blood clotting [48]. Therefore, the inhibition of the thrombus initiated by the intrinsic coagulation pathway and injury to blood vessels can be evaluated with the carrageenan-induced thrombosis model.

RG has been reported to have no significant effects on activated partial thromboplastin time, the representative evaluation of inhibitory effects on the intrinsic coagulation pathway [44], whereas PGA and Fu have been found to significantly prolong activated partial thromboplastin time [23,24]. Likewise, free RG showed no significant inhibitory effects in a carrageenan-induced thrombosis model initiated by the intrinsic coagulation pathway. Therefore, the increased activity of RG seen in the PF-NPs could be due to the presence of PGA and Fu, which might enhance the inhibitory activity even though RG alone has no effect. Furthermore, the PF-NPs showed significantly higher inhibitory activity than heparin and aspirin, the positive controls. Heparin, a sulfated glycosaminoglycan, is widely used as an anticoagulant to prevent thrombosis due to its significant antithrombotic effects. However, it has to be administered parenterally because of its poor absorption and low bioavailability in the GI tract [49]. Aspirin is also a potent anticoagulant; however, it potentially induces severe adverse effects in the GI tract, including bleeding, perforation, and inhibition of gastric cyclooxygenase activity, which is involved in cardioprotection [50]. On the other hand, PF-NPs prepared with natural compounds have potential as safe and potent anticoagulants for oral administration.

3.6. *In vivo AV shunt thrombosis model*

The control, free RG, and PF-NP groups yielded thrombus weights of 276 ± 5.5, 190 ± 5.5, and 116 ± 12.9 mg, respectively (Fig. 4c). RG showed significant inhibition of thrombus formation in the AV shunt model, and the activity significantly increased by encapsulation within the PF-NPs.

The secondary step of the blood coagulation mechanism consists of the intrinsic and extrinsic pathways, which are triggered by different inactive factors. The two coagulation pathways converge on factor Xa, which plays a role in platelet activation, leading to thrombus formation. The thrombus formation in the AV shunt model is influenced by factor Xa; therefore, the AV shunt model is regarded as the integrated evaluation method for antithrombotic activity [51]. In this study, the AV shunt model confirmed the significant thrombolytic effect of RG and the increased activity observed with PF-NPs. The results achieved with PF-NPs can be explained by the increase in stability and solubility of the ginsenosides when used in PF-NPs, as well as the complex antithrombotic activities of PGA and Fu.

3.7. *BHK 21 cell viability*

The effects of the different concentration of PF-NPs suspensions on BHK 21 cell viability were evaluated by MTT assay (Fig. 5). All cells survived after 24 h of continuous exposure to PF-NPs and viability of BHK 21 cell was not significantly influenced at PF-NPs

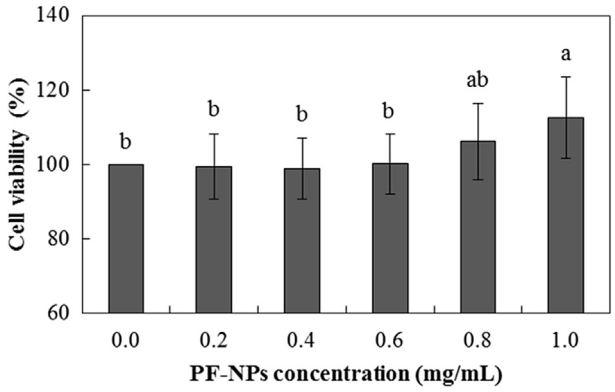

0. 5. BHK 21 cell viability of PF-NPs. All data are presented as mean ± standard deviation, and different lowercase letters indicate significant differences ($p < 0.05$). BHK 21, Baby hamster kidney fibroblast.

concentration varied from 0.2 to 0.8 mg/mL. Coating materials of PF-NPs, CS from crab shells, PGA from *Bacillus* species, and Fu from red seaweed are food-grade ingredients which are beneficial for nontoxic, biocompatible, and biodegradable properties [21,22,52]. Therefore, it can be explained that though PF-NPs were presented on nanoscale, potential toxicity induced by nano-objects was not observed due to the bioaffinity properties of its coating materials.

Moreover, the viability was significantly increased at above the 0.8 mg/mL PF-NPs. Ginsenoside derivatives, the core materials of PF-NPs are bioactive compounds which have various pharmacological activities including antioxidant and anti-inflammatory activities. Moreover, ginsenoside Rg1 was reported to increase the cell viability and decrease the cell apoptosis [53]. It can be assumed that increased concentration of bioactive ginsenoside at higher PF-NPs possibly contributed to the increase of BHK 21 cell viability. Consequentially, the results indicated that PF-NPs had no significant negative effects on cell viability.

3.8. Acute toxicity

For gross general observation including mortality, abnormal clinical signs, and changes in food consumption and body weight, significant differences between control and the administered groups were not observed ($p < 0.05$). In chemical pathological analysis, clinical chemistry parameters including GLU, blood urea nitrogen, creatinine, total protein, total cholesterol, triglyceride, aspartate aminotransferase, alanine aminotransferase, gamma glutamyl transpeptidase, alkaline phosphatase, sodium (Na), inorganic phosphorus, potassium (K), chloride (Cl), and calcium (Ca), and urinalysis parameters including pH of urine, protein, GLUu, erythrocyte, and ketone showed no significant differences between the groups ($p < 0.05$). In necropsy finding, absolute and relative organ weights and macroscopic observation of organs did not show any changes by PF-NPs administration, either ($p < 0.05$). Based on the results (data not shown), lethal dose for 50 percent kill (LD_{50}) and approximate lethal dose of PF-NPs after single oral administration in male and female rats were assumed over 3,000 mg/kg, and considered to be safe for oral application.

From these results, the contribution of the PF-NPs on RG activity can be explained by two main factors: the effect of nanoencapsulation and the complex activities of the coating materials. In this study, through the encapsulation within PF-NPs, acidic stability and solubility of ginsenosides during digestion was improved, resulting in significantly increase of antiplatelet activities inherent in RG. In addition to the conventional effects of nanoencapsulation, owing to the simultaneous anticoagulation activities of PGA and FU, PF-NPs showed a significant inhibitory effect against the intrinsic coagulation pathway that RG does not affect. Moreover, in terms of the simple and economical fabrication method and nontoxicity, PF-NPs can be suggested as a safe, effective, and industrially applicable technology for effective oral administration of RG.

Conflicts of interest

The authors declare that there are no conflicts of interest regarding the publication of this article.

Acknowledgments

This work was supported by the research fund of Hanyang University (HY-2017).

Appendix A. Supplementary data

Supplementary data to this article can be found online at https://doi.org/10.1016/j.jgr.2020.04.001.

References

[1] Heo JH, Lee ST, Chu K, Oh M, Park HJ, Shim JY, Kim M. An open label trial of Korean red ginseng as an adjuvant treatment for cognitive impairment in patients with Alzheimer's disease. Eur J Neurol 2008;15(8):865–8.
[2] Jeon BH, Kim CS, Park KS, Lee JW, Park JB, Kim K-J, Kim SH, Chang SJ, Nam KY. Effect of Korea red ginseng on the blood pressure in conscious hypertensive rats. Gen Pharmacol Vasc Syst 2000;35(3):135–41.
[3] Vuksan V, Sung M-K, Sievenpiper JL, Stavro PM, Jenkins AL, Di Buono M, Lee K-S, Leiter LA, Nam KY, Arnason JT, et al. Korean red ginseng (*Panax ginseng*) improves glucose and insulin regulation in well-controlled, type 2 diabetes: results of a randomized, double-blind, placebo-controlled study of efficacy and safety. Nutr Metab Cardiovas 2008;18(1):46–56.
[4] Furie B, Furie BC. Thrombus formation *in vivo*. J Clin Invest 2005;115(12):3355.
[5] Furie B, Furie BC. Mechanisms of thrombus formation. N Engl J Med 2008;359(9):938–49.
[6] Lee CH, Kim J-H. A review on the medicinal potentials of ginseng and ginsenosides on cardiovascular diseases. J Ginseng Res 2014;38(3):161–6.
[7] Jeon BR, Kim SJ, Hong SB, Park H-J, Cho JY, Rhee MH. The inhibitory mechanism of crude saponin fraction from Korean red ginseng in collagen-induced platelet aggregation. J Ginseng Res 2015;39(3):279–85.
[8] Kim J-H. Cardiovascular diseases and *Panax ginseng*. J Ginseng Res 2012;36(1):16–26.
[9] Kwon H-W, Shin J-H, Cho H-J, Rhee MH, Park H-J. Total saponin from Korean red ginseng inhibits binding of adhesive proteins to glycoprotein IIb/IIIa via phosphorylation of VASP (Ser 157) and dephosphorylation of PI3K and Akt. J Ginseng Res 2016;40(1):76–85.
[10] Han M. Difference in oral absorption of ginsenoside Rg1 between *in vitro* and *in vivo* models. Acta Pharmacol Sin 2006;27(4):499–505.
[11] Tawab MA, Bahr U, Karas M, Wurglics M, Schubert-Zsilavecz M. Degradation of ginsenosides in humans after oral administration. Drug Metab Dispos 2003;31(8):1065–71.
[12] Fang Z, Bhandari B. Encapsulation of polyphenols–a review. Trends Food Sci Technol 2010;21(10):510–23.
[13] Solís-Morales D, Sáenz-Hernández C, Ortega-Rivas E. Attrition reduction and quality improvement of coated puffed wheat by fluidised bed technology. J Food Eng 2009;93(2):236–41.
[14] Desai MP, Labhasetwar V, Amidon GL, Levy RJ. Gastrointestinal uptake of biodegradable microparticles: effect of particle size. Pharm Res 1996;13(12):1838–45.
[15] Fan W, Yan W, Xu Z, Ni H. Formation mechanism of monodisperse, low molecular weight chitosan nanoparticles by ionic gelation technique. Colloids Surf B Biointerfaces 2012;90:21–7.
[16] Lin N, Huang J, Dufresne A. Preparation, properties and applications of polysaccharide nanocrystals in advanced functional nanomaterials: a review. Nanoscale 2012;4(11):3274–94.
[17] Ichikawa S, Iwamoto S, Watanabe J. Formation of biocompatible nanoparticles by self-assembly of enzymatic hydrolysates of chitosan and carboxymethyl cellulose. Biosci Biotechnol Biochem 2005;69(9):1637–42.
[18] Chandramouli V, Kailasapathy K, Peiris P, Jones M. An improved method of microencapsulation and its evaluation to protect *Lactobacillus* spp. in simulated gastric conditions. J Microbiol Methods 2004;56(1):27–35.
[19] Yoo SH, Song YB, Chang PS, Lee HG. Microencapsulation of alpha-tocopherol using sodium alginate and its controlled release properties. Int J Biol Macromol 2006;38(1):25–30.

[20] Hajdu I, Bodnár M, Filipcsei G, Hartmann JF, Daróczi L, Zrínyi M, Borbély J. Nanoparticles prepared by self-assembly of chitosan and poly-γ-glutamic acid. Colloid Polym Sci 2008;286(3):343–50.
[21] Huang YC, Lam UI. Chitosan/fucoidan pH sensitive nanoparticles for oral delivery system. J Chin Chem Soc 2011;58(6):779–85.
[22] Keresztessy Z, Bodnár M, Ber E, Hajdu I, Zhang M, Hartmann JF, Minko T, Borbély J. Self-assembling chitosan/poly-γ-glutamic acid nanoparticles for targeted drug delivery. Colloid Polym Sci 2009;287(7):759–65.
[23] Hong S-P, Kim T-W, Park C, Poo H, Sung M-H. Anticoagulant and composition for preventing thrombus containing poly-gamma-glutamic acid. United States patent US 8618057B2. 2006 Dec 31.
[24] Zhu Z, Zhang Q, Chen L, Ren S, Xu P, Tang Y, Luo D. Higher specificity of the activity of low molecular weight fucoidan for thrombin-induced platelet aggregation. Thromb Res 2010;125(5):419–26.
[25] Silva E, Rogez H, Larondelle Y. Optimization of extraction of phenolics from *Inga edulis* leaves using response surface methodology. Sep Purif Technol 2007;55(3):381–7.
[26] Yoo S-H, Song Y-B, Chang P-S, Lee HG. Microencapsulation of α-tocopherol using sodium alginate and its controlled release properties. Int J Biol Macromol 2006;38(1):25–30.
[27] Kim ES, Lee J-S, Lee HG. Nanoencapsulation of red ginseng extracts using chitosan with polyglutamic acid or fucoidan for improving antithrombotic activities. J Agric Food Chem 2016;64(23):4765–71.
[28] Davidov-Pardo G, Joye IJ, McClements DJ. Encapsulation of resveratrol in biopolymer particles produced using liquid antisolvent precipitation. Part 1: preparation and characterization. Food Hydrocoll 2015;45:309–16.
[29] Kim MK, Lee J-S, Kim KY, Lee HG. Ascorbyl palmitate-loaded chitosan nanoparticles: characteristic and polyphenol oxidase inhibitory activity. Colloids Surf B Biointerfaces 2013;103:391–4.
[30] Yang J, Chen J, Pan D, Wan Y, Wang Z. pH-sensitive interpenetrating network hydrogels based on chitosan derivatives and alginate for oral drug delivery. Carbohydr Polym 2013;92(1):719–25.
[31] Jin Y-R, Yu JY, Lee J-J, You S-H, Chung J-H, Noh J-Y, Im J-H, Han X-H, Kim T-J, Shin K-S, et al. Antithrombotic and antiplatelet activities of Korean red ginseng extract. Basic Clin Pharmacol Toxicol 2007;100(3):170–5.
[32] Simkhada JR, Cho SS, Mander P, Choi YH, Yoo JC. Purification, biochemical properties and antithrombotic effect of a novel *Streptomyces* enzyme on carrageenan-induced mice tail thrombosis model. Thromb Res 2012;129(2):176–82.
[33] Jin WY, Kim S-H, Kim HK, Jang DG, Nam JB, Kang YM, Hwang BY, Kim D-S. Antiplatelet and antithrombotic effect of *Phyllostachys pubescens* leaves and Mume Fructus combination. Integr Med Res 2013;2(2):70–5.
[34] Harne S, Sharma A, Dhaygude M, Joglekar S, Kodam K, Hudlikar M. Novel route for rapid biosynthesis of copper nanoparticles using aqueous extract of *Calotropis procera* L. latex and their cytotoxicity on tumor cells. Colloids Surf B Biointerfaces 2012;95:284–8.
[35] Avadi MR, Sadeghi AMM, Mohammadpour N, Abedin S, Atyabi F, Dinarvand R, Rafiee-Tehrani M. Preparation and characterization of insulin nanoparticles using chitosan and Arabic gum with ionic gelation method. Nanomedicine 2010;6(1):58–63.
[36] Mohanraj V, Chen Y. Nanoparticles-a review. Trop J Pharm Res 2007;5(1):561–73.
[37] Dai W-G, Dong LC, Song Y-Q. Nanosizing of a drug/carrageenan complex to increase solubility and dissolution rate. Int J Pharm 2007;342(1):201–7.
[38] Gordon S, Teichmann E, Young K, Finnie K, Rades T, Hook S. *In vitro* and *in vivo* investigation of thermosensitive chitosan hydrogels containing silica nanoparticles for vaccine delivery. Eur J Pharm Sci 2010;41(2):360–8.
[39] Xu R. Progress in nanoparticles characterization: sizing and zeta potential measurement. Particuology 2008;6(2):112–5.
[40] Lahtinen M, Hölttä P, Riekkola M, Yohannes G. Analysis of colloids released from bentonite and crushed rock. Phys Chem Earth 2010;35(6):265–70.
[41] Li L, Sillanpää M, Tuominen M, Lounatmaa K, Schultz E. Behavior of titanium dioxide nanoparticles in *Lemna minor* growth test conditions. Ecotoxicol Environ Saf 2013;88:89–94.
[42] Hermawan AA, Bing TK, Salamatinia B. Application and optimization of using recycled pulp for methylene blue removal from wastewater: a response surface methodology approach. Int J Environ Sci Te 2015;6(4):267.
[43] de Clerck F, David J-L, Janssen PA. Inhibition of 5-hydroxytryptamine-induced and-amplified human platelet aggregation by ketanserin (R 41 468), a selective 5-HT_2-receptor antagonist. Agents Actions 1994;43(3–4):225–34.
[44] Yu JY, Jin Y-R, Lee J-J, Chung J-H, Noh J-Y, You S-H, Kim N-I, Im J-H, Lee J-H, Seo J-M, et al. Antiplatelet and antithrombotic activities of Korean red ginseng. Arch Pharm Res 2006;29(10):898–903.
[45] Jiao Y, Ubrich N, Marchand-Arvier M, Vigneron C, Hoffman M, Lecompte T, Maincent P. *In vitro* and *in vivo* evaluation of oral heparin–loaded polymeric nanoparticles in rabbits. Circulation 2002;105(2):230–5.
[46] Luan X, Skupin M, Siepmann J, Bodmeier R. Key parameters affecting the initial release (burst) and encapsulation efficiency of peptide-containing poly (lactide-co-glycolide) microparticles. Int J Pharm 2006;324(2):168–75.
[47] Arslan R, Bektas N, Bor Z, Sener E. Evaluation of the antithrombotic effects of *Crataegus monogyna* and *Crataegus davisii* in the carrageenan-induced tail thrombosis model. Pharm Biol 2014;53(2):275–9.
[48] Arslan R, Bor Z, Bektas N, Meriçli AH, Ozturk Y. Antithrombotic effects of ethanol extract of *Crataegus orientalis* in the carrageenan-induced mice tail thrombosis model. Thromb Res 2011;127(3):210–3.
[49] Chen M-C, Wong H-S, Lin K-J, Chen H-L, Wey S-P, Sonaje K, Lin Y-H, Chu C-Y, Sung H-W. The characteristics, biodistribution and bioavailability of a chitosan-based nanoparticulate system for the oral delivery of heparin. Biomaterials 2009;30(34):6629–37.
[50] Fiorucci S, Santucci L, Gresele P, Faccino RM, del Soldato P, Morelli A. Gastrointestinal safety of NO-aspirin (NCX-4016) in healthy human volunteers: a proof of concept endoscopic study. Gastroenterology 2003;124(3):600–7.
[51] Wong PC, Quan ML, Earl J, Watson CA, Wexler RR, Knabb RM. Nonpeptide factor Xa inhibitors: I. studies with SF303 and SK549, a new class of potent antithrombotics. J Pharmacol Exp Ther 2000;292(1):351–7.
[52] Janes KA, Fresneau MP, Marazuela A, Fabra A, Alonso MaJ. Chitosan nanoparticles as delivery systems for doxorubicin. J Control Release 2001;73(2):255–67.
[53] Zhou T, Zu G, Zhang X, Wang X, Li S, Gong X, Liang Z, Zhao J. Neuroprotective effects of ginsenoside Rg1 through the Wnt/β-catenin signaling pathway in both *in vivo* and *in vitro* models of Parkinson's disease. Neuropharmacology 2015.